Inorganic Chemistry

Article

pubs.acs.org/IC

Oxinobactin and Sulfoxinobactin, Abiotic Siderophore Analogues to Enterobactin Involving 8-Hydroxyquinoline Subunits: Thermodynamic and Structural Studies

Amaury du Moulinet d'Hardemare, Gisèle Gellon, Christian Philouze, and Guy Serratrice*

Université Joseph Fourier-Grenoble I, Département de Chimie Moléculaire, Laboratoire de Chimie Inorganique Rédox, UMR-5250, ICMG FR-2607, CNRS, BP 53, F-38041 Grenoble Cedex, France

Supporting Information

ABSTRACT: The synthesis of two new iron chelators built on the tris-L-serine trilactone scaffold of enterobactin and bearing a 8-hydroxyquinoline (oxinobactin) or 8-hydroxyquinoline-5-sulfonate (sulfoxinobactin) unit has been described. The X-ray structure of the ferric oxinobactin has been determined, exhibiting a slightly distorted octahedral environment for Fe(III) and a Δ configuration. The Fe(III) chelating properties have been examined by potentiometric and spectrophotometric titrations in methanol−water 80/20% w/w solvent for oxinobactin and in water for sulfoxinobactin. They reveal the extraordinarily complexing ability (pFe^{III} values) of oxinobactin over the p[H] range 2−9, the pFe value at p[H] 7.4 being 32.8. This was supported by spectrophotometric competition showing that oxinobactin removes Fe(III) from ferric enterobactin at p[H] 7.4. In contrast, the Fe(III) affinity of sulfoxinobactin was largely lower as compared to oxinobactin but similar to that of the ligand O-TRENSOX having a TREN backbone. These results are discussed in relation to the predisposition by the trilactone scaffold of the chelating units. Some comparisons are also made with other quinoline-based ligands and hydroxypyridinonate ligand (hopobactin).

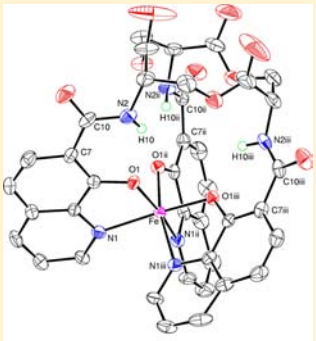

Ferric oxinobactin; pFe = 32.8 at pH 7.4

INTRODUCTION

Iron is vital for organisms; only *Lactobacillus* and *Borelia burgdoferie* bacteria are known to be iron independent.[1] Due to its very low solubility at neutral pH (~10^{-10} M, taking into account the Fe^{III}−hydroxo species[2,3]), Fe^{III} is poorly bioavailable. Thus, in order to improve Fe^{III} uptake, micro-organisms produce low molecular weight compounds called siderophores. Siderophores and most of their synthetic models contain three catechol or hydroxamic acid chelating units, giving stable Fe^{III} octahedral complexes.[4,5] Among the siderophores, enterobactin (Figure 1a) produced by *Escherichia coli* and *Salmonella typhimurium*.[6,7] exhibits the highest affinity.[8] It derives from L-serine, forming a macrocyclic trilactone framework tailoring an exceptional predisposition of its three catechol subunits for selective complexation of Fe^{III}. However, efficient synthetic chelators have been developed involving other chelating subunits.[5] Among those ligands of interest, the 8-hydroxyquinoline moiety could be considered as a hybrid between catechol and bispyridine units and possesses remarkable abilities to bind a variety of metal ions. However, curiously, it is very rarely represented in the siderophores; only *Pseudomonas fluorescens* produces a 8-hydroxyquinoline siderophore, called quinolobactin.[9] We developed the water-soluble chelator O-TRENSOX, a tris(8-hydroxyquinoline-5-sulfonate) based on the TREN scaffold, which exhibits strong complexing ability toward the ferric cation, that is of the same order of magnitude as the tris-catecholate ligands at neutral pH and is higher in acidic medium.[10,11] O-TRENSOX exhibits a selective affinity for Fe^{III}, but it is also efficient to chelate Fe^{II}, Cu^{II}, Zn^{II}, and Al^{III} in contrast to the catechol ligands.[12] Furthermore, O-TRENSOX has been found to exhibit a variety of biological properties such as iron mobilization, cell protection, and antiproliferative effects.[13] This indicates that a ligand and its ferric complex having a molecular weight of more than 1000 g mol^{-1} are able to penetrate the membranes.

Interest in synthetic siderophores includes their potential application as therapeutic iron removal agents (iron overload is one of the most common forms of metal poisoning). Moreover, there is renewed interest in this field since Fe^{3+} has been associated to Cu^{2+} and Zn^{2+} in the oxidative stress observed in amyloid plaques in Alzheimer's disease.[14] It has been reported that metal-chelating agents are able to dissolve Aβ deposits from the amyloid aggregates by removing metal ions, showing a therapeutic potential in Alzheimer's disease.[15−19] Some 8-hydroxyquinoline chelators have shown a great potential for treatment of neurodegenerative diseases.[20,21] In particular, the lipophilic metal chelator clioquinol (5-chloro-7-iodo-8-hydroxyquinoline) has been reported to dissolve amyloid plaques of the brain.[22−24] It seemed to us interesting to design a chelator possessing the most efficient organizing framework, the trilactone derived from L-serine that also confers the "chiral recognition area", but coupled to 8-hydroxyquinoline chelating subunits (Figure 1b). The aim is to obtain a ligand that is as strong as enterobactin to chelate Fe^{III} (Figure 1a) (which could eventually be recognized by its protein receptor) with improved

Received: May 23, 2012
Published: November 6, 2012

   dx.doi.org/10.1021/ic301081a | *Inorg. Chem.* 2012, 51, 12142−12151

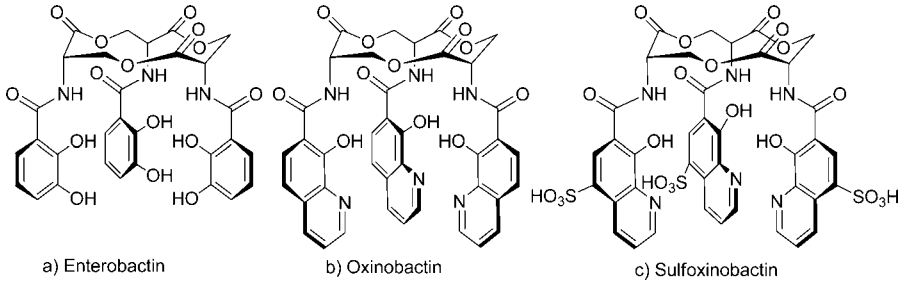

Figure 1. (a) Enterobactin (with catechol chelating subunits), (b) oxinobactin (with 8-hydroxyquinoline subunits), and (c) sulfoxinobactin (with 8-hydroxyquinoline-5-sulfonate subunits).

efficiency in acidic medium for targeting other organs (e.g., the brain is more acidic than other organs), that can form neutral iron complex (a necessity for crossing the blood–brain barrier), and that is a good chelator for Cu^{II} and Zn^{II}. To date, only one ligand built on the enterobactin scaffold and employing hydroxypyridinonate chelates (named "hopobactin") has been reported in the literature.[25]

We presented preliminary results concerning the synthesis of a novel ligand, named oxinobactin, based on the trilactone scaffold of the enterobactin and bearing three 8-hydroxyquinoline groups.[26] This paper presents an improved synthesis of oxinobactin and full characterization of the physicochemical properties of this ligand, its new sulfonated derivative (named sulfoxinobactin), and their ferric complexes, including a thermodynamic and spectrophotometric study in solution and the X-ray structure of the ferric oxinobactin.

EXPERIMENTAL SECTION

Materials and Methods. All reagents and solvents were purchased at the highest commercial quality from Acros Organics, Sigma-Aldrich, or Lancaster and used without further purification unless otherwise stated. Elemental analyses were performed by the Microanalysis Laboratory of the Département de Chimie Moléculaire. Electrospray ionization (ESI) mass spectra were recorded using an Esquire 300 Plus Bruker Daltonis. ^1H and ^{13}C NMR spectra were recorded using a Bruker Advance 300 spectrometer at 25 °C. Residual solvent signals were used as internal standard: DMSO-d_6 (^1H δ 2.49), CD_3OD (^{13}C δ 49.0), and $CDCl_3$ (^1H δ 7.24; ^{13}C δ 77). Chemical shifts in D_2O were determined relative to an internal reference of 4,4-dimethy-4-silapentane-1-sulfonic acid-d_6 (DSS) sodium salt for ^1H and ^{13}C NMR. For solubility reasons, the ligand oxinobactin and its ferric complexes were studied in a methanol/water mixture (80/20 w/w). Ionic strength was adjusted to 0.1 M with $NaClO_4$ (except for measurements over the p[H] range 0–1), and all measurements were carried out at 25.0 ± 0.2 °C. Stock solutions of Fe^{3+} were prepared by dissolving the appropriate amount of Fe^{3+} perchlorate·H_2O (~0.01 M) in 0.1 M aqueous $HClO_4$. The exact concentration of Fe^{3+} was determined spectrophotometrically using a molar extinction coefficient of 4160 M^{-1} cm^{-1} at 240 nm in 0.1 M aqueous $HClO_4$.[27] Solutions were prepared with boiled deionized water, which was deoxygenated and flushed continuously with Ar (U grade) to exclude CO_2 and O_2.

Synthesis. Oxinobactin was prepared with some modifications of our published procedures.[26] Full procedures and characterization of the precursors of oxinobactin are described in the Supporting Information. Enterobactin was prepared similarly, according to the procedures described in the ref 25 (see characterization in Supporting Information).

***N,N′,N″*-((3*S*,7*S*,11*S*)-2,6,10-Trioxo-1,5,9-trioxacyclododecane-3,7,11-triyl)-tris(8-hydroxyquinoline-7-carboxamide), Tris-hydrobromide, Oxinobactin 8.** Benzyl-protected oxinobactin 7 was synthesized according to the procedure described in the Supporting Information. To a solution of this product (1.64 g, 1.57 mmol) in dry CH_2Cl_2 (160 mL) was added BBr_3 (7.86 g, 31.3 mmol) under argon at −70 °C. After stirring overnight at 10 °C, the mixture was cooled at −70 °C and treated with methanol (40 mL) in order to hydrolyze excess of BBr_3. After stirring 2 h, solvent was evaporated. Then methanol (35 mL) and ether (20 mL) were added, and the deprotected ligand precipitated as a dark yellow solid. The mixture was filtered and dried under vacuum. The resulting product (hydrobromide form) was crystallized from methanol to afford a pale yellow powder (0.650 g, 0.639 mmol, 40%). MS (ESI) m/z: 775.1 [M − 3 HBr]$^+$. Anal. Calcd for $C_{39}H_{33}Br_3N_6O_{12}·4H_2O$: C, 42.99; H, 3.79; N, 7.71. Found: C, 42.80; H, 3.76; N, 7.50. ^1H NMR (300 MHz, DMSO-d_6/2.49): δ = 4.57 (3H, dd), 4.68 (3H, t), 5.05 (3H, dd), 7.52 (3H, d), 7.86 (3H, dd), 8.12 (3H, d), 8.66 (3H, d), 8.95 (3H, d), 9.52 (3H, d) ppm. ^{13}C NMR (75 MHz, CD_3OD/49.0): δ = 53.37 (CH), 65.14 (CH_2), 115.39 (Cq), 118.90 (CH), 125.34 (CH), 128.66 (CH), 130.78 (Cq), 132.87 (Cq), 145.72 (CH), 147.60 (CH), 154.25 (Cq), 169.65 (CO), 170.28 (CO) ppm.

***N,N′,N″*-((((3*S*,7*S*,11*S*)-2,6,10-Trioxo-1,5,9-trioxacyclododecane-3,7,11-triyl)-tris(azanediyl))-tris(carbonyl))-tris(8-hydroxyquinoline-5-sulfonic acid), Sulfoxinobactin 9.** To a CH_2Cl_2 solution (40 mL, cooled in ice) of oxinobactin trihydrobromide **8** (0.150 g, 0.147 mmol) was added chlorosulfonic acid (0.206 g, 1.76 mmol). After stirring overnight under argon at room temperature, the mixture was evaporated and the resulting residue was treated with CH_3OH and then precipitated with ether (30 mL). The precipitate was filtered and dried under vacuum. Reprecipitation from CH_3OH and ether gave sulfoxinobactin as a yellow powder (0.091 g, 0.089 mmol, 60%). MS (ESI) m/z: 1012.9 [M]$^+$. Anal. Calcd for $C_{39}H_{33}N_6O_{21}S_3·3HSO_3·2H_2O$: C, 36.11; H, 3.08; N, 6.48. Found: C, 35.94; H, 3.20; N, 6.34. ^1H NMR (300 MHz, D_2O-NaOD/DSS): δ = 3.86 (3H, d), 4.46 (6H, t), 7.52 (3H, q), 8.42 (3H, d), 8.62 (3H, d), 8.70 (3H, d) ppm. ^{13}C NMR (75.4 MHz, D_2O-NaOD/DSS): δ = 56.12 (CH), 57.99 (CH), 63.59 (CH_2), 111.57 (Cq), 119.75 (Cq), 124.22 (CH), 128.12 (Cq), 129.51 (CH), 134.87 (CH), 145.60 (Cq), 147.82 (CH), 170.32 (CO), 171.92 (Cq), 178.04 (CO) ppm.

X-ray Structure of Ferric Oxinobactin. Ferric acetylacetonate and oxinobactin were dissolved in DMF containing 5% water. The solution rapidly turned dark green and was allowed to stir for 1 h. Crystals of ferric oxinobactin were grown from diffusion of ether into the solution. Single crystals of complexes were mounted on a Kappa CCD Nonius diffractometer equipped with graphite-monochromated Mo Kα radiation (λ = 0.71073 Å) at 200 K. Reflections were corrected for Lorentz and polarization effects but not for absorption. Structures were solved by direct methods and refined using SHELXS-97 and SHELXL-97 software run under Olex2.[28] All non-hydrogen atoms were refined with anisotropic thermal parameters. Hydrogen atoms were generated at idealized positions, riding on the carrier atoms, with isotropic thermal parameters. Pertinent crystallographic data and refinement details are summarized in Table 2. Complete crystallographic data are collected in Supporting Information (CIF file format).

Potentiometric Measurements. Titrations were performed using an automatic titrator system DMS 716 Titrino (Metrohm) with a Ag/AgCl combined glass electrode (Metrohm, 6.0234.100). The electrode was filled with 3 M NaCl for measurements in water and with 0.1 M NaCl in methanol/water (80/20 w/w) for measurements in this solvent. The combined glass electrode was daily calibrated to read

dx.doi.org/10.1021/ic301081a | *Inorg. Chem.* 2012, 51, 12142–12151

Scheme 1. Synthesis of the 8-Hydroxyquinoline Fluoride Subunit 4[a]

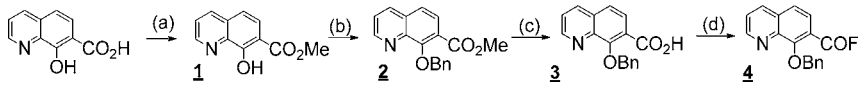

[a](a) BF_3, MeOH, reflux, 97%; (b) BnCl, K_2CO_3, H_3CCN, reflux, 95%; (c) NaOH, MeOH/THF, then pH 4−5, 80%; (d) $C_3F_3N_3$, DIPEA, CH_2Cl_2, 0 °C, 75%.

Scheme 2. Synthesis of the Trilactone Scaffold and Its Coupling with 4 to Oxinobactin 8[a]

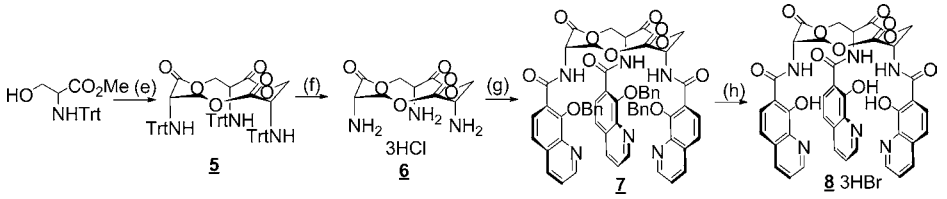

[a](e) 2,2-Dibutyl-1,3,2-dioxastannolane catalyst, toluene, reflux, 65−75%; (f) HCl, EtOH, rt, 95%; (g) **4** + DIPEA, CH_2Cl_2, 0 °C, 62%; (h) **7** + BBr_3/MeOH, −70 °C, 40%.

p[H] by titrating $HClO_4$ (0.005 M) with CO_2-free NaOH (0.01 M standardized against hydrogen phtalate) under a stream of argon. For studies in methanol/water (80/20 w/w), the calibration procedure was analogous to that in aqueous medium. The stream of argon was presaturated with methanol vapor. The GLEE program[29] was applied for glass electrode calibration and check of carbonate in the NaOH solution. The ionic product of H_2O was fixed to 13.78 in water and 14.2[30] in methanol/water mixture. The potentiometric data for the titration of the ligands (0.0005 M, p[H] range 2.7−10.5, 150 points) were refined with the HYPERQUAD program, which uses nonlinear least-squares fitting methods.[31] The standard deviation, σ, was in the range 3−4. The stability of the serine ester backbone of the ligands was checked by UV−vis spectrophotometry and ^{1}H NMR in basic medium (p[H] = 9). No change of the spectra was observed for 2 h. It was deduced that the ligands were stable during titration in the p[H] range 7−9, indicating that the rate of serine ester hydrolysis was slow enough with respect to duration of measurements.

Spectrophotometric Measurements. Titrations of the ligands (ca. 10^{-5} M) were carried out in a thermostatted cell by adding known volumes of NaOH. Emf data (converted in p[H] from calibration with GLEE program) were recorded with the DMS 716 Titrino. Absorption spectra were recorded using an optical fiber dip probe (Hellma, 661.602-UV) connected to a Varian Cary 50 UV−vis spectrophotometer.

Titrations of an equimolar solution in ligand and Fe^{3+} (ca.10^{-4} M) were done in two sets of measurements since complexation started in very acidic medium: (i) in the p[H] range 0−2, batch solutions were prepared using standardized $HClO_4$ to adjust p[H]; spectra were recorded 30 minutes after mixing the compounds to take into account the kinetics of complex formation and prevent possible hydrolysis of the trilactone scaffold in a very acidic medium (the stability of the ligands was checked by UV−vis spectrophotometry at p[H] = 0); (ii) in the p[H] range 2−10, the same procedure as the titration of the ligands was carried out. After each addition of NaOH it was ensured that complete equilibration was attained (ca. 10 minutes) before measurement of the Emf and recording the spectrum. Absorption data were processed with the SPECFIT/32 Global Analysis System (Spectrum Software Associates), adjusting the equilibrium constants and the corresponding molar extinction coefficient of the species at equilibrium.[32−34] The standard deviation σ was in the range 0.008−0.010. It should be noted that ionic strength was not maintained at 0.1 M in the p[H] range 0−1. Thus, the stability constants are less accurate.

The formation constant of the ferric sulfoxinobactin was also determined by competition against Na_2H_2EDTA over the p[H] range 1.9−2.8 (4 solutions). Typical solutions were 10^{-4} M in ferric ion, ligand, and Na_2H_2EDTA. The p[H] of the solutions was adjusted by addition of $HClO_4$ and $NaClO_4$ to maintain the ionic strength at 0.1 M. Samples were allowed to equilibrate for 72 h at 25 °C.

RESULTS AND DISCUSSION

Syntheses. Synthesis of the oxinobactin is realized by following the general plan adopted during our previous work to which we brought some modification and improvement, leading to a more reliable procedure.[26] It is a convergent synthesis in which the first part consists in preparing the fluoride of the 8-hydroxyquinoline acid **4** by protecting beforehand in two steps the phenol function by a benzyl group (Scheme 1).

The fluoration step is best done with cyanuric fluoride, which gives better yield and a better purity than the more popular DAST fluorinating reagent. It must be pointed out that the fluoride **4** is stable enough to be purified by the conventional chromatography procedure, in contrast to its chloride homologue which decomposes readily. The second part of this convergent synthesis aims at preparation of the trilactone of L-serine **6**, a key compound in the synthesis, and its coupling with the fluoride **4** (Scheme 2).

Starting from methyl L-serinate from which the nitrogen is beforehand protected by the trityl group (methyl L-trityl serinate is also commercially available), the key reaction of macrolactonization is realized with the 2,2-dibutyl-1,3,2-dioxastannolane taken as the best organostannic catalyst tested (75% yield). Later, after deprotection of **5** by hydrochloric acid, the macrolactone **6** is coupled with the fluoride **4**, affording the benzylic-protected oxinobactin **7** with a satisfactory yield of 62%. Removal of benzyl groups by hydrogenation catalyzed by palladium on charcoal gives over-reduction of the quinoline nucleus, and only 16% of oxinobactin **8** could be recovered after a very tedious step of chromatography. Improved results were obtained with BBr_3 as the debenzylating agent, which raised the yield to 40%. The purification was also simplified because the tris-hydrobromide so obtained could be easily purified by crystallization from methanol instead the more difficult step of chromatography. The sulfoxinobactin **9** derives from oxinobactin **8** by direct sulfonation. The usual sulfonating oleum (30% SO_3 in H_2SO_4) proved to be unsatisfactory; only decomposition products ensued. In contrast, good results were obtained with chlorosulfonic acid in 12 mol excess in dry

dx.doi.org/10.1021/ic301081a | Inorg. Chem. 2012, 51, 12142−12151

dichloromethane: in this condition the yield is 62% (Scheme 3).

Scheme 3. Sulfonation of Oxinobactin[a]

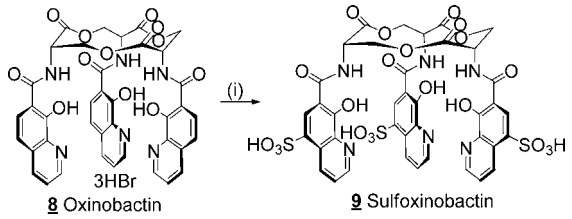

[a](i) HSO_3Cl, CH_2Cl_2, 62%.

Protonation of the Ligands. Since the metal ions compete with the protons for the coordination sites, it is necessary to determine the acid–base properties of the ligands. The ligands oxinobactin and sulfoxinobactin, denoted $L^1H_6^{3+}$ and L^2H_6, respectively, in the fully protonated form, possess six potential protonation sites: three phenolate oxygen atoms and three pyridinyl nitrogen atoms (the sulfonate groups in L^2H_6 are assumed to be deprotonated under the conditions of titration). The protonation equilibria, defined by eq 1

$$LH_{n-1} + H \overset{K_n}{\rightleftharpoons} LH_n \text{(charges are omitted)} \quad (1)$$

were studied by potentiometric titration in the p[H] range 2.7–10.5 (i) for $L^1H_6^{3+}$ in methanol/water (80/20 w/w, I = 0.1 M $NaClO_4$) owing to its poor solubility in water (Figure 2) and

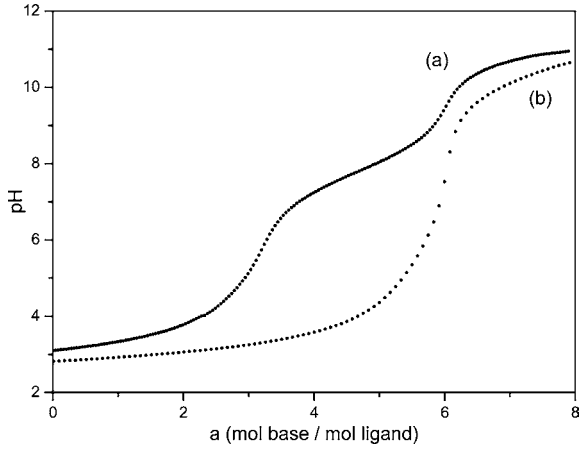

Figure 2. Potentiometric titration curves: (a) 4.5 × 10^{-4} M oxinobactin, (b) [oxinobactin]/[Fe^{3+}] = 1/1, 4.5 × 10^{-4} M. Solvent: CH_3OH/H_2O (80/20 w/w), I = 0.1 M ($NaClO_4$), T = 25.0(2) °C.

(ii) for $L^2H_6^{3+}$ in water (I = 0.1 M $NaClO_4$) (Figure S1, Supporting Information). Data were analyzed by the HYPERQUAD program.[31] An additional study using a UV–vis spectrophotometric titration was performed using the SPECFIT program[32–34] for fitting analysis of the absorbance data. For $L^1H_6^{3+}$, the potentiometric study revealed five protonation constants (the number in parentheses corresponds to the standard deviation): log K_1 = 8.51(3), log K_2 = 7.78(2), log K_3 = 6.90(4), log K_4 = 4.02(7), and log K_5 = 2.75(9). Spectrophotometric titration was carried out in the p[H] range 1.7–9.3. Two buffer regions were observed, one in the p[H] range 1.7–5.7 (Figure 3a, spectra exhibit isosbestic points at 258 and 286 nm) and the other in the p[H] range 6.7–9.3

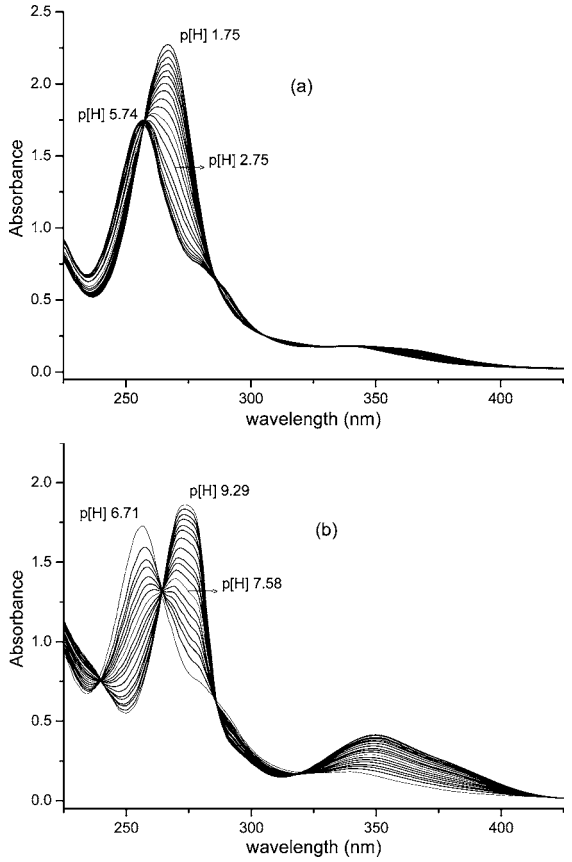

Figure 3. UV–vis absorption spectra of oxinobactin (2.0 × 10^{-5} M) as a function of p[H]: (a) p[H] = 1.75, 1.82, 1.88, 1.92, 1.98, 2.03, 2.08, 2.16, 2.24, 2.44, 2.58, 2.75, 2.98, 3.11, 3.40, 3.65, 3.91, 4.16, 4.90, and 5.74; (b) p[H] = 6.71, 6.84, 7.00, 7.12, 7.31, 7.58, 7.72, 7.82, 7.90, 8.03, 8.17, 8.30, 8.40, 8.54, 8.71, 8.89, and 9.29. Solvent: CH_3OH/H_2O (80/20 w/w), I = 0.1 M ($NaClO_4$), T = 25.0(2)°C.

(Figure 3b, spectra exhibit isosbestic points at 240, 264, and 286 nm). Analysis of the data by the SPECFIT program[32–34] gave a model with only two absorbing species involving one proton exchange in each p[H] range. Calculation yields two values of protonation constants: 2.28(2), which were attributed to log K_6, and 7.64(2). This last value is in good agreement with log K_2 = 7.78(2) determined by potentiometric titration.

For L^2H_6, potentiometric titration allowed us to determine only four protonation constants log K_1 = 7.84(1), log K_2 = 7.03(1), log K_3 = 6.18(2), and log K_4 = 2.78(4). In complement with this study, we undertook a spectrophotometric titration in the p[H] range 1–8. Two buffer regions were observed, one in the p[H] range from 1 to 2.8 (Figure S2a, Supporting Information, spectra exhibit isosbestic points at 251 and 273 nm) and the other from p[H] 5 to 7 (Figure S2b, Supporting Information, spectra exhibit isosbestic points at 242, 256, and 277 nm). Treatment of the absorbance data by the SPECFIT program indicated the presence of only two absorbing species corresponding to one proton exchange in each p[H] range 1.0–2.8 and 4.7–7.8 and gave values of 1.42(3) and 5.99(3) attributed to log K_6 and log K_3, respectively. This last value favorably agrees with log K_3 = 6.18 determined by potentiometric titration. In addition, the value of log K_5 was estimated to be 2 for calculation of the Fe(III) stability constants.

dx.doi.org/10.1021/ic301081a | Inorg. Chem. 2012, 51, 12142–12151

Table 1. Protonation Constants[a] of Oxinobactin ($L^1H_6^{3+}$), Sulfoxinobactin (L^2H_6), and Ligands Containing 8-Hydroxyquinoline Subunits

ligand	log K_1	log K_2	log K_3	average log K_{1-3}	log K_4	log K_5	log K_6	average log K_{4-6}
oxinobactin[b]	8.51(3)	7.78(2)	6.90(4)	7.73	4.02(7)	2.75(9)	2.28(2)	3.02
sulfoxinobactin[c]	7.84(1)	7.03(1)	6.18(2)	7.02	2.78(4)	~2	1.42(3)	2.07
COX2000[c,d]	10.38	8.40	6.80	8.53	4.13	2.89	2.43	3.15
O-TRENSOX[c,e]	8.62	8.18	7.44	8.08	3.01	2.55	1.83	2.46
n-Busox (Q^{S4})[c,f]	6.80	2.80						
Q^{S10}[c,g]	6.77	2.60						

[a]Numbers in parentheses represent the standard deviation in the last significant digit. [b]In methanol/water (80/20 w/w, I = 0.1 M $NaClO_4$). [c]In water (I = 0.1 M $NaClO_4$). [d]Reference 35. [e]Reference 11. [f]Reference 36, 8-hydroxy-7-[(butylamino)carbonyl]quinoline-5-sulfonic acid. [g]Reference 37, 8-hydroxy-7-[(decylamino)carbonyl]quinoline-5-sulfonic acid.

Scheme 4. Structures of *n*-Busox, Q^{S10}, O-TRENSOX, COX200, and COX2000

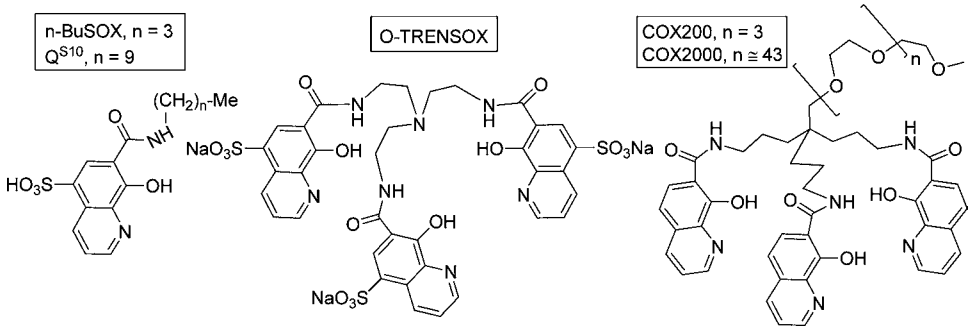

All constants are reported in Table 1 together with those of ligands containing 8-hydroxyquinoline (COX2000,[35] based on a C-pivot scaffold grafted with a polyoxyethylenic chain) or 8-hydroxyquinoline-5-sulfonate units (O-TRENSOX,[11] based on the backbone of tris(2-aminoethyl)amine, n-Busox,[36] Q^{S10}[37]); see structures in Scheme 4.

The constants K_1–K_3 are attributed to protonation of the phenolate oxygen atoms and constants K_4–K_6 to the pyridinyl nitrogen atoms. In spite of the difference of solvents, the log K of $L^1H_6^{3+}$ and L^2H_6 can be compared: the average value for the log K of the oxygen sites, 7.02 for L^2H_6, is lower than the corresponding value, 7.73 for $L^1H_6^{3+}$, in relation to the electron-withdrawing effect of the sulfonate group. The same trend is observed for protonation of the nitrogen sites: the average values are 2.07 and 3.02 for L^2H_6 and $L^1H_6^{3+}$, respectively. The log K ranges for the nitrogen and oxygen atoms differ from the statistical factor of log 3 (0.48), indicating that there is some cooperativity between the three arms of the ligands. The average values of the log K_{4-6} and log K_{1-3} for L^2H_6, 7.02 and 2.07, can be compared to the log K values of the monochelate analogues n-Busox (6.80 and 2.80)[36] and Q^{S10} (6.77 and 2.60)[37] (Table 1). The log K values can also be compared to those of tripodal ligands containing three 8-hydroxyquinoline chelating subunits (Table 1). The log K values of oxinobactin $L^1H_6^{3+}$ are similar to those determined in aqueous solution for the tris(chelate) analogue COX2000 (Scheme 4), except for log K_1, which is abnormally high for COX2000.[35] The log K values of sulfoxinobactin L^2H_6 are lower than those of O-TRENSOX (average values of log K_1–K_3 = 8.08 and log K_4–K_6 = 2.46).[11] The higher values for O-TRENSOX could be due to an extended network of H bonding involving the nitrogen atom of the tripodal backbone.

The electronic spectrum of oxinobactin in its protonated form is characterized by a strong absorption band at higher energies (267 nm, ε = 1.3 × 10^5 M^{-1} cm^{-1}) and a broad band at 360 nm (ε = 8.8 × 10^3 M^{-1} cm^{-1}). Deprotonation of the pyridine nitrogen results in hypsochromic shifts (256 nm, ε = 8.7 × 10^4 M^{-1} cm^{-1}; 340 nm, ε = 9.4 × 10^3 M^{-1} cm^{-1}), while deprotonation of the phenol group leads to bathochromic and hyperchromic shifts as expected (274 nm, ε = 9.4 × 10^4 M^{-1} cm^{-1}; 350 nm, ε = 2.1 × 10^4 M^{-1} cm^{-1}). The changes of the band at higher energies of sulfoxinobactin (267 nm, ε = 8.0 × 10^4 M^{-1} cm^{-1}) are different from that of oxinobactin: bathochromic shift upon deprotonation of pyridine nitrogen (280 nm, ε = 5.8 × 10^4 M^{-1} cm^{-1}) and hypsochromic shift upon deprotonation of the phenol group (268 nm, ε = 7.4 × 10^4 M^{-1} cm^{-1}) as it has been already observed by the sulfonated ligands n-Busox[36] and Q^{S10}.[37]

X-ray Structure of Ferric Oxinobactin. Single crystals of the Fe^{III}–oxinobactin complex [$Fe(C_{39}H_{27}N_6O_{12})$] were obtained by diffusion of diethyl ether into a solution of the complex in DMF containing 5% water. The complex crystallizes in the $R3$ rhomboedral space group with Z = 3 (Table 2). The structure reveals a neutral mono-Fe^{III} complex having C_3 symmetry and a slightly distorted octahedral tris(8-hydroxyquinolinate) environment for Fe^{III} (Figure 4). Owing to the 3-fold symmetry axis, only one-third of a molecule unit is necessary to be crystallographically described. Each 8-hydroxyquinolinate subunit forms a 5-membered chelate ring with iron, leading to the facial isomer (Figure 4b). As we can judge it by observing the crystallographic structure of the complex, the trilactone scaffold still presents the *S* configuration for carbons 3, 7, and 11, brought by the L-serine (no racemization occurred during synthesis). As the configuration of the ligand imposes that of the metallic center, we indeed observe a right-handed configuration (Δ chirality) as is the case for the ferric enterobactin. Selected bond lengths and angles are reported in Table 3. The five-membered chelate ring angle O1–Fe–N1 is 79.1°, whereas the other cis angles are 98.4° for O1–Fe–N1ii, 92.4° for both O1–Fe–O1ii and O1–Fe–O1iii,

dx.doi.org/10.1021/ic301081a | *Inorg. Chem.* 2012, 51, 12142–12151

Table 2. Crystallographic Data for Ferric Oxinobactin

formula	$[Fe(C_{39}H_{27}N_6O_{12})]\cdot dmf$
fw [g·mol^{-1}]	827.54 + dmf
color/morphology	blue prism
cryst size	0.35 × 0.21 × 0.18
cryst syst	trigonal
space group	*R*3
a [Å]	18.650(1)
b [Å]	18.650(1)
c [Å]	12.317(2)
α [deg]	90
β [deg]	90
γ [deg]	120
unit-cell volume [Å^3]	3710.2(8)
D_x (g·cm^{-3})	1.406
T [K]	200
Z	3
λ [mm^{-1}]	0.71073
total reflns	8841
unique reflns (Friedel's included)	3716
obsd reflns	3384 ($F^2 > 2\sigma$)
R_{int}	0.0482
R^a	0.0532
$R(w)^a$	0.1262
goodness of fit *S*	1.125
$\Delta_{min}\rho/\Delta\rho_{max}$ (e·Å^{-3})	−0.56/0.54

[a]Refinement based on F^2 where $w = 1/[\sigma^2(F_o^2) + 0.0548p^2 + 10.9877p]$ and $p = (F_o^2 + 2F_c^2)/3$ for **2**·3THF.

91.7° for both N1−Fe−N1ii and N1−Fe−N1iii, and 166.5° for the apical O1−Fe−N1iii angle. These angles are in the range observed for Fe−COX200 (ligand with the same structure as COX2000 but with a shorter polyoxyethylenic chain, see Scheme 4).[34] The trigonal twist angle (60° for an ideal octahedron) has been calculated to be 43.9°.[38] This value is less distorted from octahedral geometry than the values for hopobactin (35°) or enterobactin (estimated 33°),[25] indicating there are less steric constraints with the 8-hydroxyquinolinate chelates.

Table 3. Selected Bond Lengths (Angstroms) and Angles (degrees) for Fe−Oxinobactin

Fe−O1	1.949(2)	O1−Fe−N1 chelate	79.1
Fe−N1	2.166(3)	O1−Fe−N1ii cis	98.4
N2···O1	2.69	O1−Fe−O1	92.4
H10···O1	2.04	N1−Fe−N1	91.7
N2−H10−O1	129.7	O1−Fe−N1iii apical	166.5

The oxygen and nitrogen atoms of the amide group are slightly displaced from the quinoline plane: the dihedral angle between O2−C10−C7 or N2−C10−C7 and the quinoline plane is 166.2° or 11.6°, respectively. The Fe−O and Fe−N distances are 1.949 and 2.166 Å, respectively. These values are identical to the average distances 1.948 and 2.164 Å observed for the Fe−Cox200.[35] Interestingly, the structure reveals that the amide protons interact strongly by hydrogen bonding with the quinolinol oxygens coordinated to iron, forming three 6-membered rings. The H10···O1 and N2···O1 distances are 2.04 and 2.69 Å, respectively, and the angle NHO is 129.7°. This hydrogen bonding is an important feature of the structure and contributes to enhance the stability of the complex. This interaction is also observed in Fe^{III} triscatecholate: as an example, for [Fe(TRENCAM)] the H···O distances vary from 1.80 to 1.85 Å.[39]

In summary, these results underline the ability of the enterobactin scaffold to bring chelate units more bulky than catecholamide, such 8-hydroxyquinoline, leading to ferric complex with less distorted octahedral geometry. Furthermore, the structures of the ferric COX200 complex having a C-pivot tripodal backbone and the ferric oxinobactin complex show very close coordination geometry (bonds and dihedral angles), although the ligands have very different structures of their backbone.

Stability Constants of the Ferric Complexes. Potentiometric titration was carried out for 1:1 solutions in ferric ion and ligand from p[H] 2. The curves (Figures 2b and S1b, Supporting Information, for ferric−oxinobactin and ferric−sulfoxinobactin, respectively) showed an inflection at a = 6, indicating that the six protons of the ligand have been displaced

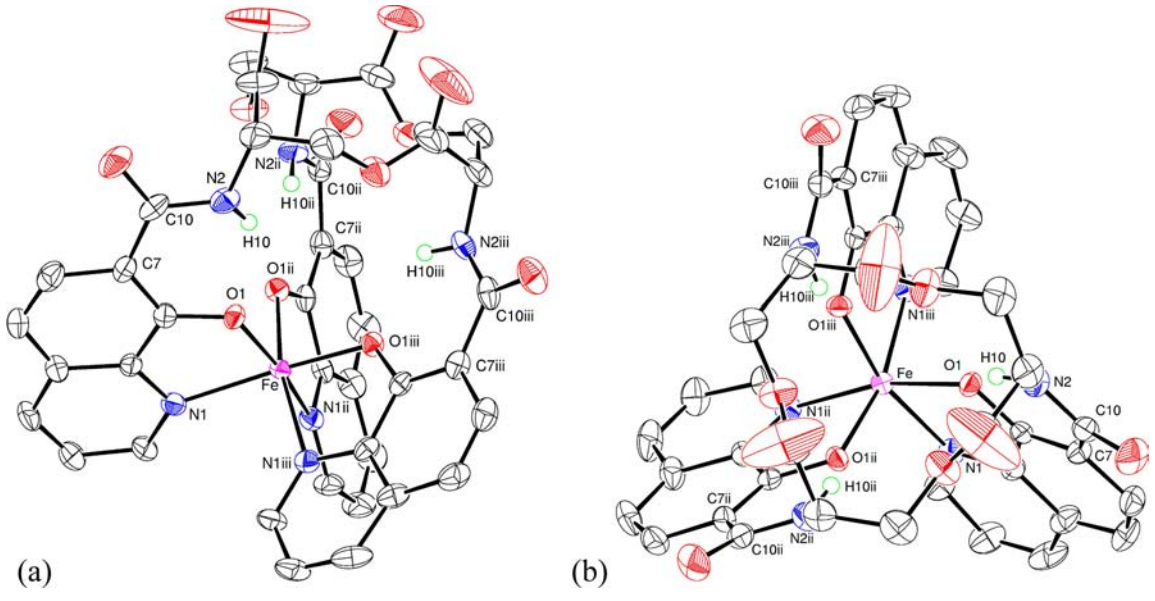

Figure 4. ORTEP diagram at 25% probability of the ferric oxinobactin viewed perpendicular to (a) and down (b) the molecular 3-fold axis.

dx.doi.org/10.1021/ic301081a | *Inorg. Chem.* 2012, 51, 12142−12151

by the ferric ion. Furthermore, comparison of the curves for the ligand and its ferric complex indicates that hydroxo complexes were formed at p[H] above about 9 for ferric oxinobactin and about 8 for ferric sulfoxinobactin. Since the ferric complex is fully formed at p[H] 2, formation equilibria were studied by spectrophotometric titration of equimolar solutions of ferric ion and ligand. First, a set of solutions in the p[H] range 0−2 was studied at variable molar concentrations of standardized $HClO_4$. Second, a spectrophotometric−p[H] titration was carried out from p[H] 2 to 9.

For the two complexes, an increase of p[H] from 0 to 2 led to the growth of charge-transfer bands centered at 440 and 590 nm (Figure 5 and Figure S3, Supporting Information). The best

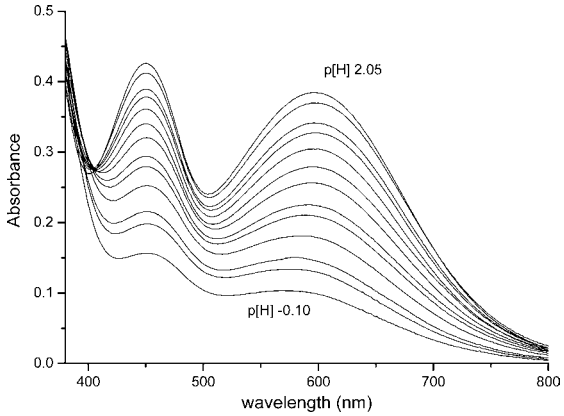

Figure 5. UV−vis absorption spectra of Fe^{3+}−oxinobactin at p[H] = −0.10, −0.01, 0.04, 0.22, 0.46, 0.56, 0.64, 0.94, 1.16, 1.42, 1.62, and 2.05. $[Fe^{3+}] = 8.9 \times 10^{-4}$ M, [oxinobactin] = 9.7×10^{-5} M. Solvent: CH_3OH/H_2O (80/20 w/w), I = 0.1 M ($NaClO_4$), T = 25.0(2) °C.

refinement of the absorbance−p[H] data with the program SPECFIT was obtained by considering formation of the $FeL^nH_3^{3+}$ and FeL^n species. The global stability constants β_{11h} of these complexes, which are defined by eqs 2 and 3, are reported in Table 4. It should be noted that the values of log

Table 4. Equilibrium Constants log β_{11h} and UV−Vis Data of Ferric Complexes with Oxinobactin (L^1) and Sulfoxinobactin (L^2)

complex[a]	log $\beta_{11\,h}$	λ/nm (ε, 10^3 M^{-1} cm^{-1})	pFe^{III}[b]
$[FeL^1H_3]^{3+}$	36.75 (5)	450 (3.8), 585 (2.8)	
$[FeL^1]$	33.61 (13)	450 (4.8), 600 (4.3)	32.8
$[FeL^2H_3]$	30.66 (5)	430 (4.0), 575 (2.6)	
$[FeL^2]^{3-}$	26.73 (9)	430 (5.8), 580 (4.4)	27.1
$[FeL^2OH]^{4-}$	18.68 (2)	425 sh, 530 (1.9)	
[Fe(COX2000)][c]	32.12	450 (4.6), 590 (3.9)	29.1
[Fe(O-TRENSOX)][3−d]	30. 9	443 (5.4), 595 (5.4)	29.5

[a]Measurements in methanol/water (80/20 by weight) for the Fe−L^1 system and water solutions for other complexes, I = 0.1 M $NaClO_4$. [b]pFe^{III} = −log $[Fe^{3+}]$ calculated for $[Fe]_{tot} = 10^{-6}$ M, $[L]_{tot} = 10^{-5}$ M, and p[H] = 7.4. [c]Reference 35. [d]Reference 11.

β_{113} are less accurate than the other constants because the ionic strength varied over the p[H] range 0−1 (charges are omitted).

$$Fe^{3+} + L^n + hH^+ \rightleftharpoons FeL^nH_h \quad (2)$$

$$\beta_{11h} = [FeL^nH_h]/[Fe^{3+}][L^n][H^+]^h \quad (3)$$

No spectral change was observed over the p[H] range 2−9 (Figure S5, Supporting Information) for ferric oxinobactin and 2−6 for ferric sulfoxinobactin (Figure S6, Supporting Information). For this last complex, a change of the absorption was observed over the p[H] range 6−9, indicating formation of hydroxo complexes (Figures S4 and S6, Supporting Information). Spectra exhibited isosbestic points at 330 and 420 nm. Analysis of the absorbance−p[H] data provided formation of the hydroxo species FeL^2OH. The complexation constant is reported in Table 4.

The stability constant β_{110} of the ferric complex FeL^2 was also determined by spectrophotometric competition experiments with ethylenediaminetetraacetic acid (edta) over the p[H] range 1.9−2.8 (Figure 6). The existence of isosbestic

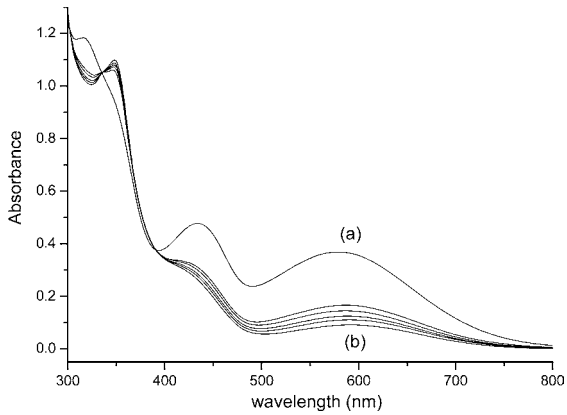

Figure 6. Spectrophotometric competition of ferric sulfoxinobactin in the presence of EDTA at p[H] = 2.47; [Fe sulfoxinobactin] = [EDTA] = 8.3×10^{-5} M ; T = 25 °C. Spectra were recorded at t (min) = 0 (a) and 1, 3, 10, 20, and 180 (b) after mixing solutions of ferric sulfoxinobactin and EDTA.

points at 325 and 410 nm suggest that no ternary Fe−EDTA−L^2 complex was formed. The competition equilibrium can be expressed by eqs 4 and 5, in which Y denotes edta, K_1−K_3 denote the protonation constants of L^2H_3, and K_1', K_2', and K_3' denote the protonation constants of YH_3.[40]

$$FeL^2 + YH_3 \rightleftharpoons FeY + L^2H_3 \quad (4)$$

$$K = [FeY][LH_3]/[FeL][YH_3] = \beta_{110(FeY)}K_1K_2K_3/\beta_{110(FeL)}K_1'K_2'K_3' \quad (5)$$

The concentration of FeL^2 was calculated from the absorbance at 590 nm, where FeL^2 is the only absorbing species. The concentrations of the other species in eqs 4 and 5 were calculated from the mass balance equation and p[H] (eqs 6−8) in which α is the usual Ringbom coefficient.[41]

$$[Fe]_{tot} = \alpha_{FeL}[FeL^2] + \alpha_{FeY}[FeY] \quad (6)$$

$$[L^2]_{tot} = \alpha_{FeL}[FeL^2] + \alpha_L[L^2] \quad (7)$$

$$[Y]_{tot} = \alpha_{FeY}[FeY] + \alpha_Y[Y] \quad (8)$$

From the known formation constants of FeY (log β_{110} = 25.1[40] the average formation constant of FeL^2 was determined to be log β_{110} = 26.5 ± 0.2. This value is in good agreement with the value 26.7, determined from spectrophotometric titration.

The two bands exhibited by the visible spectra of the FeL^1 complex at 450 (ε = 4800 M^{-1} cm^{-1}) and 595 nm (ε = 4300

dx.doi.org/10.1021/ic301081a | Inorg. Chem. 2012, 51, 12142−12151

M^{-1} cm^{-1}) and of the FeL^2 complex at 430 (ε = 5800 M^{-1} cm^{-1}) and 580 nm (ε = 4400 M^{-1} cm^{-1}) are characteristic of the tris(8-hydroxyquinolinate) coordination as observed with the FeL species of the ferric COX2000[35] and O-TRENSOX[11] complexes. The spectral characteristics of the FeL^1H_3 complexes, two bands at 450 (ε = 3800 M^{-1} cm^{-1}) and 585 nm (ε = 2800 M^{-1} cm^{-1}), and of FeL^2H_3, two bands at 430 (ε = 4000 M^{-1} cm^{-1}) and 575 nm (ε = 2600 M^{-1} cm^{-1}), suggest coordination of two 8-hydroxyquinoline moieties having one protonated hydroxyl group and one free protonated 8-hydroxyquinoline ligand. It should be noted that no salicylate coordination (through the oxygen atoms of the hydroxyl and carbonyl groups) was observed in acidic medium, in contrast to Fe−COX2000 and Fe−O-TRENSOX. Salicylate coordination is characterized by a strong band at 440−445 nm and a shoulder near 550 nm.[11] Salicylate coordination has been also evidenced for ferric enterobactin. In contrast, no salicylate coordination has been observed for ferric hopobactin.[25] The spectral parameters of the FeL^2OH species suggest coordination with one 8-hydroxyquinoline unit. The remaining coordination sites are thus occupied by four water molecules to complete the octahedral geometry, one of the water molecules being deprotonated to give a hydroxyl anion. A value of 8.05 is calculated from β_{110} and β_{11-1} for $pK_a(FeL^2OH/FeL^2)$. This value is too high to be attributed to hydroxyl deprotonation of a free arm of the ligand,

Spectrophotometric Competition with Enterobactin. Since no data are available for ferric enterobactin equilibria in methanol−water solvent, it was interesting to compare the efficiency of oxinobactin relative to enterobactin toward Fe^{III} in this solvent at physiological pH. For this aim, we carried out a spectrophotometric competition in MOPS methanol−water buffer (p[H] = 7.4). Spectra are depicted in Figure 7. The

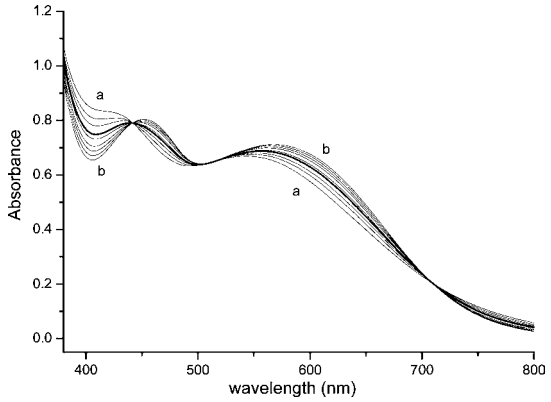

Figure 7. Spectrophotometric competition of ferric enterobactin in the presence of oxinobactin at p[H] = 7.3, [MOPS] = 0.05 M, [Fe−enterobactin] = [oxinobactin] = 1.6×10^{-4} M, T = 25 °C. Spectra were recorded at t (min) = 1 (a) and 180 (b).

spectrum of the ferric enterobactin in this buffer exhibits a band at 505 nm (ε = 4800 M^{-1} cm^{-1}). After addition of 1 equiv of oxinobactin to a solution of ferric enterobactin (Figure 7), the spectra showed fast growth of bands at 450 and 580 nm that are characteristic of the ferric oxinobactin. After 3 h the spectra did not change and were similar to that of the ferric oxinobactin. This clearly shows that oxinobactin completely remove Fe^{III} from ferric enterobactin. The same experiment was realized with sulfoxinobactin in a MOPS aqueous buffer. Spectra recorded after mixing of ferric enterobactin and sulfoxinobactin solutions showed no change. This experiment confirms that sulfoxinobactin is less efficient than enterobactin to chelate Fe^{III}, in agreement with the pFe values.

Since the ligands are weak acids, proton competition occurs depending on their protonation and the pH. The pFe^{III} value ($pFe^{III} = -\log [Fe^{3+}]$) is thus a better measure of the relative efficiency of the ligands under given conditions of pH, $[Fe]_{tot}$, and $[L]_{tot}$. The pFe^{III} values have been calculated for $[L]_{tot} = 10^{-5}$ M, $[Fe]_{tot} = 10^{-6}$ M, and p[H] over the range 2−9. In spite of the difference of solvents, one can compare the plots of pFe^{III} vs p[H] for oxinobactin (Figure 8) and COX2000 (pFe

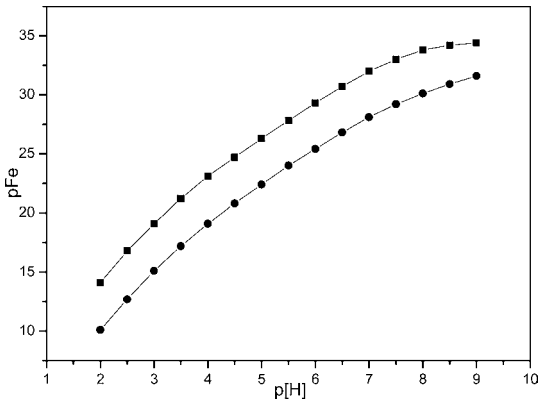

Figure 8. Plot of pFe versus p[H]. pFe = $-\log [Fe^{3+}]$ calculated for $[Fe]_{tot} = 10^{-6}$ M, $[L]_{tot} = 10^{-5}$ M: (■) oxinobactin and (●) COX2000.

values were calculated from complexation constants determined in aqueous solution)[35] to gain insight into the effect of the scaffold structure on complex stability. An increase of about 4 log units is observed over the pH range 2−9 on going from COX2000 to oxinobactin, showing that the trilactone scaffold induces a large increase of the efficiency of the ligand for metal binding. A similar comparison between the "TREN-capped" ligands and the derivatives of the enterobactin reveals an increase varying from 8.7 (pH = 4) to 5.5 (pH = 9) log units in the pFe values between TRENCAM[42] and enterobactin[8] (catecholate binding units) (Figure S7, Supporting Information), whereas the difference between TRENHOPO and hopobactin (pyridinonate binding units) (Figure S7, Supporting Information) is about 4 log units over the pH range 2−6 but only 0.7 at pH 7.4.[25] It should be noticed that oxinobactin is the most efficient Fe(III) chelator in acidic and neutral pH. It has been claimed that the very high affinity for ferric ion of enterobactin is largely due to the predisposition of the catecholamide units induced by the trilactone ring, thus allowing one to reduce the energy to bind the cation. The enhanced affinity of oxinobactin for ferric ion with respect to COX2000 and the very similar coordination geometry around the iron for these two ferric complexes provide support to the ability of the 8-hydroxyquinoline moieties to be predisposed with the trilactone scaffold in spite of their bigger bulkiness than that of the catechol groups. This is also consistent with the structure of the ferric oxinobactin, which reveals a relatively small degree of steric strain as indicated by the twist angle of 43.9°. In contrast, no enhancement of affinity for ferric ion is evidenced between sulfoxinobactin and O-TRENSOX[11] from the plot pFe−pH (Figure S8, Supporting Information). It can be inferred that sulfonate substituents do not favor the predisposition of the chelating groups by the trilactone scaffold.

dx.doi.org/10.1021/ic301081a | Inorg. Chem. 2012, 51, 12142−12151

CONCLUSION

Two new analogs of the enterobactin have been synthesized: the one lipophilic having 8-hydroxyquinoline groups (oxinobactin) and the other hydrophilic having 8-hydroxyquinoline-5-sulfonate groups (sulfoxinobactin). The X-ray structure of the ferric oxinobactin complex indicates C_3 symmetry and slight distortion from the octahedral geometry having the Δ configuration. An interesting comparison can be made between the ferric complexes of oxinobactin and the ligands COX200 or COX2000 having the same chelating units and a C-pivot tripodal scaffold grafted with a polyoxyethylenic chain, n = 3 or 45, respectively.[35] The geometry around the iron cation is very similar (distances and angles), indicating that the interaction between the cation and the donor groups is of similar magnitude for these two ligands. This suggests that the scaffold structure has no effect on the interaction strength between the chelating units and the iron cation. Furthermore, the efficiency of the iron complexation, measured by the pFe, is enhanced by 4 pFe units between COX2000 (having a longer polyoxyethylenic chain than COX200 allowing solubility in water) and oxinobactin over the pH range 2−9. This suggests that the predisposition of the chelating units is responsible for the gain in stability of ferric oxinobactin over ferric COX2000. However, no gain in stability is observed for the 8-hydroxyquinoline-5-sulfonate chelating units by comparison of sulfoxinobactin and O-TRENSOX[11] having a TREN scaffold. Our results provide additional evidence of the extraordinary ability of the trilactone scoffold of enterobactin to predispose a great variety of chelating units for selective and strong complexation of the ferric ion and highlight the interest for ligands having the 8-hydroxyquinoline moiety. Other complexing subunits can be so intended to be transplanted, bringing additional properties as fluorescence for intracellular localization of the iron.

ASSOCIATED CONTENT

Supporting Information

Synthesis of oxinobactin precursors; X-ray crystallographic data in CIF format for ferric oxinobactin; figures showing potentiometric and spectrophotometric titrations of sulfoxinobactin and its ferric complexes; figures showing a plot of the absorbance at λ_{max} vs p[H] for Fe−oxinobactin and Fe−sulfoxinobactin; figures showing pFe vs pH for various ligands. This material is available free of charge via the Internet at http://pubs.acs.org.

AUTHOR INFORMATION

Corresponding Author

*E-mail: guy.serratrice@ujf-grenoble.fr.

Notes

The authors declare no competing financial interest.

REFERENCES

(1) Crichton, R. R. In *Inorganic Biochemistry of Iron metabolism*; John Wiley & Sons: Chichester, 2001.
(2) Kragter, J. *Atlas of Metal-Ligand Equilibria in Aqueous Solution*; Halstead Press: New York, 1978.
(3) Boukhalfa, H.; Crumbliss, A. L. *BioMetals* **2002**, *15*, 325−339.
(4) Telford, J. R.; Raymond, K. N. Siderophores. In *Comprehensive Supramolecular Chemistry*; Atwood, J. L., Davies, J. E. D., MacNicol, D. D., Vögtle, F., Eds.; Elsevier Science Ltd.; Oxford, 1996, Vol. *1*; pp 245−266.
(5) Albrecht-Gary, A.-M.; Crumbliss, A. L. In *Metal Ions in Biological Systems*; Sigel, A., Sigel, H., Eds.; Marcel Dekker; New York, 1998, Vol. *35* (Iron Transport and Storage in Microorganisms, Plants and Animals), pp 239−327.
(6) O'Brien, J. G.; Gibson, F. *Biochim. Biophys. Acta* **1970**, *215*, 393−402.
(7) Pollack, J. R.; Neilands, J. B. *Biochem. Biophys. Res. Commun.* **1970**, *38*, 989−992.
(8) Loomis, L. D.; Raymond, K. N. *Inorg. Chem.* **1991**, *30*, 906−911.
(9) Mossialos, D.; Meyer, J. M.; Budzikiewicz, H. P. *Appl. Environ. Microbiol.* **2000**, *66*, 487−492.
(10) Baret, P.; Beguin, C.; Boukhalfa, H.; Caris, C.; Laulhère, J.-P.; Pierre, J.-L.; Serratrice, G. *J. Am. Chem. Soc.* **1995**, *117*, 9760−9761.
(11) Serratrice, G.; Boukhalfa, H.; Beguin, C.; Baret, P.; Caris, C.; Pierre, J.-L. *Inorg. Chem.* **1997**, *36*, 3898−3910.
(12) Biaso, F.; Baret, P.; Pierre, J.-L.; Serratrice, G. *J. Inorg. Biochem.* **2002**, *89*, 123−130.
(13) Pierre, J.-L.; Baret, P.; Serratrice, G. *Curr. Med. Chem.* **2003**, *10*, 1077−1084.
(14) Bush, A. I. *Trends Neurosci.* **2003**, *26*, 207−214.
(15) Boldron, C.; Van der Auwear, I.; Deraeve, C.; Gornitzka, H.; Wera, S.; Pitié, M.; Van Leuven, F.; Meunier, B. *ChemBioChem* **2005**, *6*, 1976−1980.
(16) Cui, Z.; Lockman, P. R.; Atwood, C. S.; Hsu, C.-H.; Gupte, A.; Allen, D. D.; Mumper, R. J. *Eur. J. Pharm. Biopharm.* **2005**, *59*, 263−272.
(17) Cherny, R. A.; Barnham, K. J.; Lynch, T.; Volitakis, I.; Li, Q.-X.; McLean, C. A.; Multhaup, G.; Beyruether, K.; Tanzi, R. E.; Masters, C. L.; Bush, A. I. *J. Struct. Biol.* **2000**, *130*, 209−216.
(18) Dedeoglu, A.; Cormier, K.; Payton, S.; Tseitlin, K. A.; Kremsky, J. N.; Lai, L.; Li, Q.-X.; Moir, R. D.; Tanzi, R. E.; Bush, A. I.; Kowall, N. W.; Rogers, J. T.; Huang, X. *Exp. Geront.* **2004**, *39*, 1641−1649.
(19) Lee, J.-Y.; Friedman, J. E.; Angel, I.; Kozak, A.; Koh, J.-Y. *Neurobiol. Aging* **2004**, *25*, 1315−1321.
(20) Deraeve, C.; Pitie, M.; Mazarguil, H.; Meunier, B. *New J. Chem.* **2007**, *31*, 193−195.
(21) Deraeve, C.; Boldron, C.; Maraval, A.; Mazarguil, H.; Gornitzka, H.; Vendier, L.; Pitié, M.; Meunier, B. *Chem.—Eur. J.* **2008**, *14*, 682−696.
(22) Cherny, R. A.; Atwood, C. S.; Xilinas, M. E.; Gray, D. N.; Jones, W. D.; McLean, C. A.; Barnham, K. J.; Volitakis, I.; Fraser, F. W.; Kim, Y. S.; Huang, X. D.; Goldstein, L. E.; Moir, R. D.; Lim, J. T.; Beyreuther, K.; Zheng, H.; Tanzi, R. E.; Masters, C. L.; Bush, A. I. *Neuron* **2001**, *30*, 665−676.
(23) Ritchie, C.; Bush, A. I.; Mackinnon, A.; Macfarlane, S.; Mastwyk, M.; McGregor, L.; Kiers, L.; Cherny, R. A.; Li, Q.-X.; Tammer, A.; Carrington, D.; Mavros, C.; Volitakis, I.; Xilinas, M.; Ames, D.; Davis, S.; Beyreuther, K.; Tanzi, R. E.; Masters, C. L. *Arch. Neurol.* **2003**, *60*, 1685−1691.
(24) Bush, A. I. *Neurobiol. Aging* **2002**, *23*, 1031−1038.
(25) Meyer, M.; Telford, J. R.; Cohen, S. M.; White, D. J.; Xu, J.; Raymond, K. N. *J. Am. Chem. Soc.* **1997**, *119*, 10093−10103.
(26) du Moulinet d'Hardemare, A.; Alnaga, N.; Serratrice, G.; Pierre, J.-L. *Bioorg. Med. Chem. Lett.* **2008**, *18*, 6476−6478.
(27) Bastian, R.; Weberling, R.; Palilla, F. *Anal. Chem.* **1956**, *28*, 459−462.
(28) Sheldrick, G. M. *SHELXS-97, Program for crystal structure solution*; University of Göttingen: Göttingen, Germany, 1997. Sheldrick, G. M. *SHELXL-97, Program for the refinement of crystal structures*; University of Göttingen: Göttingen, Germany; 1997. Dolomanov, O. V.; Bourhis, L. J.; Gildea, R. J.; Howard, J. A. K.; Puschmann, H. *J. Appl. Crystallogr.* **2009**, *42*, 339−341.
(29) Gans, P.; O'Sullivan, B. *Talanta* **2000**, *51*, 33−37.
(30) Rochester, C. H. *Dalton Trans.* **1972**, 5−8.
(31) Gans, P.; Sabatani, A.; Vacca, A. *Talanta* **1996**, *43*, 1739−1743.
(32) Gampp, H.; Maeder, M.; Meyer, C. J.; Zuberbühler, A. D. *Talanta* **1985**, *32*, 95−101.
(33) Gampp, H.; Maeder, M.; Meyer, C. J.; Zuberbühler, A. D. *Talanta* **1985**, *32*, 257−264.
(34) Gampp, H.; Maeder, M.; Meyer, C. J.; Zuberbühler, A. D. *Talanta* **1986**, *33*, 943−951.

(35) Imbert, D.; Baret, P.; Gaude, D.; Gautier-Luneau, I.; Gellon, G.; Thomas, F.; Serratrice, G.; Pierre, J.-L. *Chem.—Eur. J.* **2002**, *8*, 1091−1100.
(36) Launay, F.; Alain, V.; Destandau, E.; Ramos, N.; Bardez, E.; Baret, P.; Pierre, J.-L. *New J. Chem.* **2001**, *25*, 1269−1280.
(37) Brandel, J.; Torelli, S.; Gellon, G.; Serratrice, G.; Putaux, J.-L.; Pierre, J.-L. *Eur. J. Inorg. Chem.* **2009**, 86−92.
(38) The trigonal twist angle is defined by viewing the N3−N3ii−N3iii and O1−O1ii−O1iii planes in a projection perpendicular to the 3-fold axis of the complex. It is calculated as the dihedral angle O1−D1−D2−N3 (D1 and D2 are the centers of the N3−N3ii−N3iii and O1−O1ii−O1iii triangles).
(39) Stack, T. D. P.; Karpishin, T. B.; Raymond, K. N. *J. Am. Chem. Soc.* **1992**, *114*, 1512−1514.
(40) Martell, A. E.; Smith, R. M. *Critical Stability Constants*; Plenum Press: New York, 1974; Vol. *1*.
(41) Ringbom, A. *Complexation in Analytical Chemistry*; Interscience Publisher: New York, 1963.
(42) Rodgers, S. J.; Lee, C.-W.; Ng, C. Y.; Raymond, K. N. *Inorg. Chem.* **1987**, *26*, 1622−1625.